Talanta 259 (2023) 124468

Contents lists available at ScienceDirect

Talanta

journal homepage: www.elsevier.com/locate/talanta

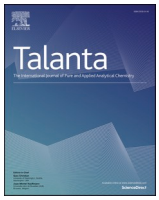

Direct, precise, enzyme-free detection of miR-103–3p in real samples by microgels with highly specific molecular beacons

Sabrina Napoletano [a], Edmondo Battista [d], Nicoletta Martone [c], Paolo Antonio Netti [a,b,c], Filippo Causa [a,b,c,*]

[a] Interdisciplinary Research Centre on Biomaterials (CRIB), Università degli Studi di Napoli "Federico II", Piazzale Tecchio 80, 80125 Naples, Italy
[b] Dipartimento di Ingegneria Chimica del Materiali e della Produzione Industriale (DICMAPI), University "Federico II", Piazzale Tecchio 80, 80125 Naples, Italy
[c] Center for Advanced Biomaterials for Healthcare@CRIB, Istituto Italiano di Tecnologia (IIT), Largo Barsanti e Matteucci 53, 80125 Naples, Italy
[d] Department of Innovative Technologies in Medicine & Dentistry, University "G. d'Annunzio" Chieti-Pescara, Via dei Vestini, 31, 66100, Chieti, Italy

ARTICLE INFO

Handling Editor: J.-M. Kauffmann

Keywords:
miRNAs detection
Biosensor
Microgel
Sensitivity
Real-sample

ABSTRACT

Low abundance, small size, and sequence similarities render microRNA (miRNAs) detection challenging, particularly in real samples, where quantifying weakly expressed miRNAs can be arduous due to interference of more abundant molecules. The standard quantitative reverse transcription polymerase chain reaction (qRT-PCR) requires multiple steps, thermal cycles, and costly enzymatic reactions that can negatively affect results. Here we present a direct, precise, enzyme-free assay based on microgels particles conjugating molecular beacons (MB) capable of optically detecting low abundant miRNAs in real samples. We validate the applicability of microgels assay using qRT-PCR as a reference technology. As a relevant case, we chose miR-103–3p, a valuable diagnostic biomarker for breast cancer, both in serum samples and MCF7 cells. As a result, microgels assay quantifies miRNA molecules at room temperature in a single step, 1 h (vs. 4 hrs for qRT-PCR) without complementary DNA synthesis, amplification, or expensive reagents. Microgels assay exhibits femtomolar sensitivity, single nucleotide specificity, and a wide linear range (10^2–10^7 fM) (wider than qRT-PCR), with low sample consumption (2 μL) and excellent linearity (R^2= 0.98). To test the selectivity of the microgel assay in real samples, MCF7 cells were considered where the pool of 8 other miRNAs were further upregulated with respect to miRNA 103–3p. In such complex environments, microgels assay selectively detects the miRNA target, mainly due to MB advanced stability and specificity as well as high microgel antifouling properties. These results show the reliability of microgels assay to detect miRNAs in real samples.

1. Introduction

microRNAs (miRNAs)-guided diagnostics could become a powerful molecular approach for deriving clinically significant information from patient samples [1,2]. Recently miR-103–3p was described as a diagnostic and prognostic marker in several diseases, including several cancers [3] and Alzheimer's disease [4]. It has also been associated with the prognosis of brain stroke [5]. So, the simple and fast evaluation of circulating miR-103–3p, alone or in combination with other biomarkers, could represent an essential tool for clinical applications. However, miRNAs only represent 0.01% of total RNA mass and need to be detected from highly complex media; in blood plasma, the concentration of miRNAs is in the sub-picomolar (pM) range [6]. Therefore, miRNA molecules are considered insufficient for clinical applications, primarily due to the lack of large-scale validation and inconsistencies among detection devices [7–9], affected by assay variability and non-standardized statistical analyses. The different miRNA expression profiles obtained from polymerase chain reaction (PCR)-based methods currently used for miRNA quantification often lead to discrepancies in the abundance of miRNAs [10]. In addition, weak signals caused by low miRNA abundance in biofluids decrease the signal-to-noise ratio and complicate the measurement of rare miRNAs [11].

Quantitative reverse-transcription PCR (qRT-PCR) is currently the standard for quantitating miRNAs abundance [12]; despite it being very sensitive, qRT-PCR for miRNAs can be labor-intensive and time-consuming, requiring an elaborated reverse transcription reaction

* Corresponding author. Interdisciplinary Research Centre on Biomaterials (CRIB) , Università degli Studi di Napoli "Federico II" , Piazzale Tecchio 80 , 80125 Naples , Italy.
E-mail address: causa@unina.it (F. Causa).

https://doi.org/10.1016/j.talanta.2023.124468
Received 2 December 2022; Received in revised form 13 March 2023; Accepted 16 March 2023
Available online 23 March 2023

that already provides enzyme and gene-specific biases [13,14], followed by amplification, with consequently unreliable specificity [15]. The reason for qRT-PCR's poor performance also resides in PCR inhibition by stabilizers or by impurities that co-purify with samples. qRT-PCR inhibition is the most common cause of qRT-PCR failure when adequate copies of the target are present [16,17]. In most molecular tools for nucleic acids analyses, the inhibition by nucleic acid extracts is a well-known phenomenon; for instance, ethylenediaminetetraacetic acid (EDTA), commonly used in elution buffers for nucleic acids, can produce various degrees of inhibition. The effects of these inhibitors can range from partial inhibition and underestimation of the target nucleic acid amount to complete amplification failure [18]. Inhibitors can affect enzymes used in the reaction for miRNAs analyses (DNA polymerase and reverse transcriptase), the chelation of necessary co-factors, or can interfere with primers binding [19,20]. Moreover, relying qRT-PCR on exponential amplification, biases, and errors are amplified exponentially. A hypothetical 3% per cycle bias in a 30-cycle PCR would develop a >2-fold quantitative error; this is problematic when disease diagnosis relies on miRNAs differential expression [20]. This unaccounted uncertainty from PCR efficiency estimates entails uncontrolled false positive rates that are a significant problem in using qRT-PCR as a diagnostic tool [21–25].

As a result, there is a need to develop analytical platforms for detecting and quantifying miRNAs in complex biological samples, ideally without reverse transcription and amplification; however, it still needs to be solved, especially keeping the same sensitivity and specificity as qRT-PCR.

New biosensing techniques can provide many advantages in the detection of miRNAs; already exists a suite of tools enabled by DNA nanotechnology, the most relying on nucleic acid probes hybridizing [26,27]. Generally, biosensors have several advantages, such as low price, flexibility, portability, ease of use, fast analysis, short reaction time, speed, uncomplicated operations, robustness, reproducibility, long-term stability, minimal need for sample pretreatment, miniaturization, and on-site/in situ analysis [28]. However, in many cases, biosensors-based technologies, despite declaring to reach a limit of detection of low femtomolar (fM), need to incorporate amplification strategies (enzymes-based or enzyme-free) or temperature steps to detect the presence of low-abundant targets [29–32] or while maintaining sensitivity, they lack specificity being unable to discriminate a single nucleotide polymorphism (SNP) [33,34]. Moreover, the performances of biosensors depend on the environment where they measure, and the limit of detection (LOD) of many biosensors still needs to be defined in complex biological samples [35]. We have already described a biosensing approach for detecting miRNAs based on fluorescently labeled microgels particles conjugated with DNA probes [36–38]. The use of microgels with the fluorescent signal confinement of the specific probes into a small volume allows them to perform ultrasensitive direct target detection, avoiding complicated sample preparation and enzymatic reactions such as reverse transcription into complementary DNA and amplification (Fig. 1).

We demonstrate that the assay has a LOD down to about 10 fM in PBS with a spiked synthetic target and is easily tunable over a wide range of target concentrations (10 fM – 10 nM) using MB probes [38]. MB is a dual-labeled oligonucleotide probe with a fluorescent dye at one end and a fluorescence quencher at the opposite end. MB includes a target-specific hybridization domain (loop) between short sequences (stem) that are self-complementary and emits a fluorescence that is proportional to the amount of target in the analyzed sample. Using microgels conjugated with MB, the emitted light from the microgels sensing assay can be directly measured to quantify the target. Moreover, microgels demonstrated selectivity of 1 nucleotide that is difficult to achieve using other methods. Because of its sensitivity, selectivity, and ease of use, we propose a microgels-based assay as an excellent candidate to overcome the issues of miRNAs detection in real samples for clinical purposes. Although we have already demonstrated the accuracy of a microgels-based detection system [36,38], our previous studies didn't investigate the analytical performance of this method in real samples and the influence of a complex matrix on the reliability of our approach, in particular, to define if microgels sensing assay can represent a valid alternative to PCR-based assays.

Here, we validate the microgels assay in real biological samples for the first time. Furthermore, a new molecular beacon probe (MB) to be conjugated on microgels for a fluorescent emission is proposed for sensitive and specific detection of miR-103–3p, prognostic and diagnostic markers of breast cancer. With this scope, we evaluated the performances of microgels assay in RNA extracted from serum samples and MCF7 breast cancer cells with up-regulated miRNAs other than the analyte and compared results with qRT-PCR. While we have previously demonstrated detection using microgels-based assay, we emphasize that this work represents the first example of detecting miRNA from true biological samples. As relevant results, we demonstrate microgels assay as a reliable method for detecting miRNAs from samples with a high rate of interferents. The proposed assay is competitive with the qRT-PCR technique for precision, linearity, and trueness and can eliminate limitations of enzymatic assays reducing risks of sample contamination during the detection process.

Here we considerably validate microgel assay as a user-ready, low-cost, specific, and sensitive technology to detect and quantify miRNAs from a small amount (2 μL) of RNA extracts in one step, without

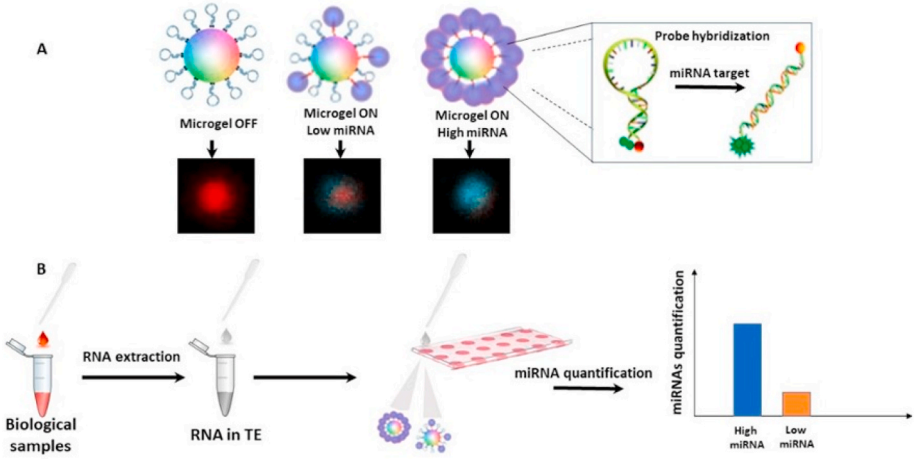

Fig. 1. Microgels assay workflow: A) Microgels in the detection of miRNA target by Molecular Beacon probe B) Microgels assay steps for miRNAs quantification in the real samples.

laborious protocol and sophisticated laboratory supplies, and in as little as 1 h. This study takes microgels assay one step closer to practical biosensing applications by demonstrating detection from biological samples and could help bring miRNA detection to everyone's fingertips with mix-and-read innovative reagents.

2. Experimental

2.1. Probe design

To achieve high specificity in identifying miR-103–3p, the MB probe was suitably designed according to alignment studies and the simulation of thermodynamic parameters. We evaluated the specificity of the probe in silico using the Primer-BLAST tool (https://blast.ncbi.nlm.nih.gov). Using bioinformatic analyses, we assessed the specificity of the probe by carrying out the probe sequence's alignment with the target sequence miR-103–3p and with the human transcriptome. The Raw Score (S) alignment data and the E-value (expected value) demonstrate a high specificity of the MB for the selected target and, consequently, of the test. The thermodynamic parameters (melting temperature, stability, and folded fraction at the dosage conditions) were calculated using appropriate tools (OligoAnalyzer 3.1; IDT- Integrated, D.N.A. 2014 and Oligocalc). Gibbs free energy (ΔG) of MB hybridization to the target was calculated to allow stable matching between the probe strand and the target at physiological ionic strength. The correct folding of the probe and hybridization to the target were evaluated through the UNAFold web server.

2.2. Microgels synthesis

Microgels labeled with the ATTO532 fluorophore were synthesized via free-radical pre-precipitation polymerization [35]. Briefly, sub-micrometer particles were obtained by mixing PEGDMA 1% (w/v), Acrylic Acid (0.034 mM), and ATTO532-maleimide dye (0.0094 mM) in PVA 1% (w/v). KPS (2.2 mM) was used as the initiator, and polymerization was conducted at a constant temperature of 65° C for 6 h under an N_2 atmosphere. Subsequently, microgels with ATTO532 fluorophore were dialyzed for 15 days, purified several times by centrifugation (for 15 min at 6500 rpm) to remove unreacted monomer, oligomers, and surfactants, and then stored at 4°C until further use. The microgel size, zeta potential, conductivity, and electrophoretic mobility were characterized by dynamic light scattering (DLS) (Malvern Zetasizer Nano ZS instrument, 633 nm laser, 173° scattering angle). The content of carboxylic groups on microgels was quantified by potential titration before the conjugation of the MB.

2.3. MB bioconjugation to microgels

MB probes with the fluorescent dye (ATTO647 N) to the 5′-end and a fluorescence quencher (BBQ-650) to the 3′-end, were conjugated to microgels labeled with the fluorophore ATTO532. Bioconjugation was optimized by coupling 0.25 nmol of the MB. Briefly, 1 mg of microgels was incubated in 250 μL of 2-(N-morpholino)ethanesulfonic acid (MES) at pH 6, whereas MB was incubated in 50 μL MES pH 6 for at least 5 h. Then, the carboxylic groups on the microgel were activated using 0.5 M of the coupling agent 1-Ethyl-3-(3-dimethylaminopropyl) carbodiimide (EDC) by stirring vigorously briefly and leaving them in ice for 20 min. Subsequently, MB solution was added to the microgels by incubating overnight at 300 rpm at 4 °C. Microgels conjugated with MB were washed three times to remove the unreacted MB and suspended in tris-(2-idrossimetil)-amminometano cloridrato (TRIS) 0.1 M. Unconjugated and conjugated microgels were characterized by DLS (dynamic light scattering). Briefly, the Z-potential and size of microgels with ATTO532 fluorophore, unconjugated and conjugated with 0.25 nmol of MB, were measured by dispersing microgels in H_2O, PBS, KCl 10^{-3} M or Tris-EDTA (pH 8) at a concentration of 50 μg/mL. A total of three runs, each comprising three cycles, were conducted (Table S2), results are the mean of the three runs.

2.4. Spectrofluorometer characterization

Fluorescence recovery by spectrofluorometer (DUETTA-HORIBA scientific) was measured at a concentration of 25 μg/mL of microgels with ATTO532 fluorophore and conjugated with 0.25 nmol of MB in TRIS-EDTA (TE). ATTO532 fluorescence was measured at an excitation wavelength of 524 nm; an emission range from 540 nm to 600 nm, an excitation and emission bandpass of 5 nm, an integration time of 0.05 s, a detector accumulation of 1, and an emission increment of 0.5 nm (1 pixel). ATTO 647 fluorescence was measured at an excitation wavelength of 647 nm; an emission range from 600 nm to 750 nm, an excitation and emission bandpass of 3 nm, an integration time of 0.2 s, a detector accumulation of 1, and an emission increment of 1 nm (2 pixels). For both fluorophore, three repetitions were made. The fluorescence of ATTO647N was moreover recorded during a temperature ramp starting from 75∘C (opened MB) and decreasing temperature to 25∘C (closed MB) (Figure S2), results are the mean of three runs.

2.5. Microgels-sensing assay calibration curve

For the final assay were used 0.5 μg/mL (corresponding to 1.45×10^7 microgels) of microgels, conjugating 0.25 nmol of MB probe. The assay was performed by mixing the microgels (with ATT0532 fluorophore and conjugated with MB) to the target sequences, without preliminary steps of amplification. A calibration curve was done plotting the fluorescence of microgels over serial dilutions of synthetic miR-103–3p in TE. The samples were analyzed by confocal microscopy with an objective 63 × 1.40 oil (Zeiss) using lasers 543 and 633 nm. Power lasers and detector gains were always kept constant with a scan speed of 8000 Hz. For each target concentration, 20 images were collected and analyzed. Images were processed and analyzed by ImageJ software. The assay for each concentration of miR-103–3p took about 1 h and was done in triplicate. Data are from 5 sets of 3 independent tests. To estimate LOD, 20 replicates of the blank sample (microgels without miR-103–3p target) were measured [39].

2.6. Reverse transcriptase and quantitative polymerase chain reaction (qRT-PCR)

For the qRT-PCR assay, 2 μL of the sample at different concentrations was reverse transcribed using the TaqMan ™ Advanced miRNA cDNA Synthesis Kit - Thermo Fisher Scientific. In detail, the mature miRNA sequence was extended using 3′ poly-A tailing and 5′ ligation of an adaptor sequence. For cDNA synthesis, universal RT primers were used to recognize the universal sequences on both the 5′ and 3' extended ends of the mature miRNAs. All mature miRNAs in the sample were reverse-transcribed to cDNA. Then 5 μL of cDNA was used as a template for Taq Man Advanced miRNA Assay - cDNA was tested in triplicate. The Taq-Man PCR was performed with the following protocol: 95 °C for 20 s, followed by 40 cycles of 95 °C for 3 s and 60 °C for 30 s. The CFX-96 real-time thermal cycler (Bio-Rad Laboratories, Inc., Hercules, CA, USA) was amplified. A calibration curve was done using serial dilutions of synthetic miR-103–3p in TE.

2.7. Detection of miR-103–3p in human serum

We tested the capability of both microgels assay and qRT-PCR to detect miR-103–3p in purified RNA from human serum (Sigma-Aldrich). Freshly thawed human serum (50 μL) was spiked with different concentrations of miR-103–3p (10 fM – 10^5 fM and 500 fM as the last point), and full miRNA content was extracted using miRNeasy Serum/Plasma Kit (Qiagen) according to the manufacturer's protocol and increasing the elution time to 5 min. Microgels assay and qRT-PCR were performed

in the same sample using the previously described protocols. Three different spiked samples (biological replicates) were tested for each concentration, results represent the mean of three different technical replicates for each sample. qRT-PCR were compared with those from the calibration curve in TE in Fig. 5 (black squares). qRT-PCR data are reported as Ct (cycle threshold) values (Fig. 5) and as ΔCt values normalized on endogenous control miR-16–5p (Fig. S4).

2.8. Detection of extracellular miR-103–3p in MCF7 cells

Cells were plated at a density of 20.000 cells/cm^2 in flasks of 75 and grown in culture medium (MEM, 10% FBS, 1% L-GLUT, 2% P/S). Once they reached the confluence of 80–90%, corresponding to about 1×10^7 cells, the culture was left in cell culture medium without serum (MEM, 1% L-GLUT, 2% P/S) for 48 h, then cell culture medium was harvested for the analysis. To isolate miRNAs, 1 mL of culture medium was processed with 700 μL of Trizol; the aqueous phase was then purified using the mirVana™ miRNA Isolation Kit from Thermo Fisher Scientific. Before extraction samples were spiked with 1 μL of 1 nM Cel-miR-39–3p synthetic miRNA, to check the correct extraction and purification procedure. The extracts were measured using a Nanodrop 2000 spectrophotometer. Both microgels assay and qRT-PCR were performed on RNA extract from MCF7 cells media as previously described. Three MCF7 samples (biological replicates) were tested. For each miRNA, the qRT-PCR and microgels assay were performed in triplicate, data represent the mean of three different technical replicates.

3. Data analysis and statistical analysis

All results from the microgels sensing assay and qRT-PCR are expressed as the mean of three different experiments; each sample was tested in triplicate. The coefficient of variation (CV) was calculated for each miRNA concentration in three replicates of one sample and was considered non-informative if CV $\geq$ 4%.

Data were analyzed using by student t-test, and only statistically significant as $p < 0.05$ were considered.

4. Results and discussion

The most widely used method for miRNA analysis relies on qRT-PCR. However, despite promising findings, qRT-PCR tests present severe limitations in their clinical application due to their technical variability [40]. Despite its high sensitivity, qRT-PCR suffers biases due to sample reverse-transcription and amplification and remains a costly and laborious assay. In the last few years, various innovative analytical methods have been implemented for circulating miRNA determination. However, a simple, low-cost, and rapid assay, which could be routinely used in clinical practice, is still required [27].

This study aimed to explore the performance of microgel sensing assay for miRNAs in terms of sensitivity, specificity, and tolerance to interferents in real samples compared with qRT-PCR. The proposed assay presents many advantages over qRT-PCR: minimal sample handling, reduced bench and reaction time, and closed-tube reactions, thanks to direct detection of the target without reverse transcription and amplification (Fig. 2).

The microgels assay is based on microgels particles conjugated with an MB that emits a fluorescence proportional to the amount of target present in the analyzed sample. To ensure the analytical performances of the microgels assay, we first checked MB hybridization to its target. MB for miR-103–3p presented challenges in design:(i) loop interference; complementary loop nucleotides hybridize with each other, thus making folded conformation more stable and less accessible by the target analyte. (ii) stem-loop hybridization; separating the fluorophore from the quencher. Due to these issues, the folding free energy of the MB predicted structure is not negative enough to guarantee the stability for MB closing (ΔG = −3.00 kcal/mol) (Fig. S1). To have the optimal MB, we

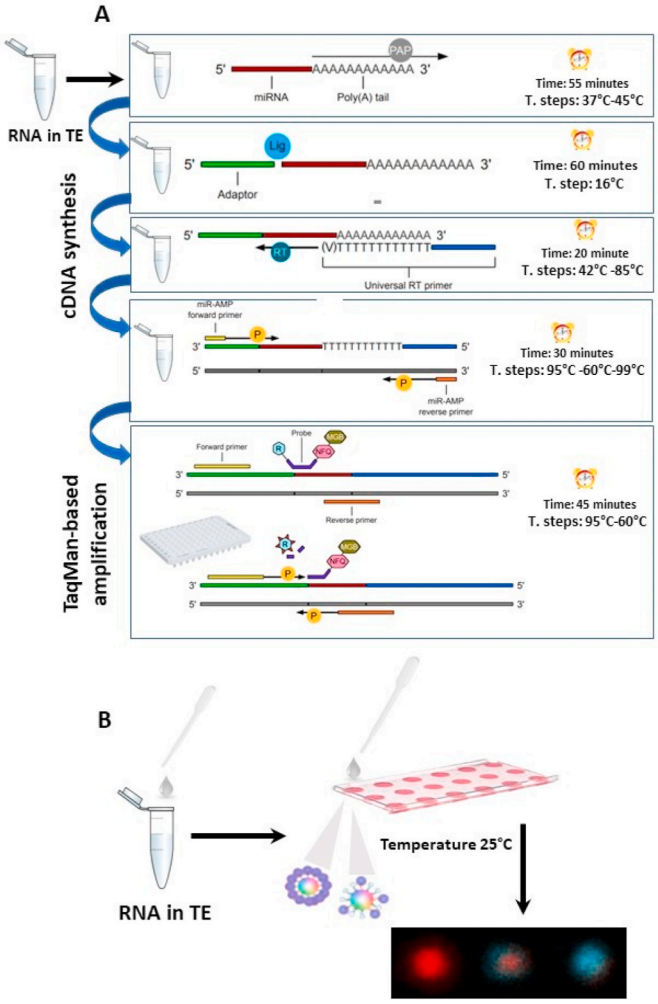

Fig. 2. Comparison of qRT-PCR and microgels assay. A) Steps of qRT-PCR to perform miRNAs quantification. B) Steps of microgels assay to perform miRNAs quantification.

made an addition of bases (ATA) between the stem and the loop (Fig. 3), overcoming the challenges of design and decreasing MB folding free energy (ΔG = −5.75 kcal/mol) (Table S1).

Furthermore, MB hybridization free energy (ΔG = -30.9 kcal/mol) shows that miR-103-3p detection occurs spontaneously at 25°C (Table S1). MB efficiency was further verified experimentally by temperature steps to test the proper folding of the MB before and after conjugation to microgels (Fig. S2). After MB conjugation on microgels, we calibrated the microgels assay (Fig. 4A and Fig. S3) and the qRT-PCR assay with serial dilutions of synthetic miR-103-3p, spiked in TE, as the target analyte (Fig. 5).

Black squares represent different serum samples spiked with different concentrations of miR-103–3p (10 fM – 10^5 fM and 500 fM as the last point) detected by qRT-PCR and compared with those from the calibration curve in TE. Three different spiked samples (biological replicates) were tested for each concentration; the results represent the mean of three different technical replicates for each sample. Error bars are SEM (standard error of the mean). In the figure, the linear regression equation and the coefficient of correlation (R^2) are shown.

Our data show that the calibration curve performed using the RNA target has a good regression coefficient for microgel assay ($R^2 = 0.98$) (Fig. S3). The calibration curve demonstrates that microgels assay can properly detect miR-103–3p at the ionic strength of TE, which is the eluting buffer used to dissolve nucleic acids after extraction from real samples and to protect them from degradation. In comparison, we

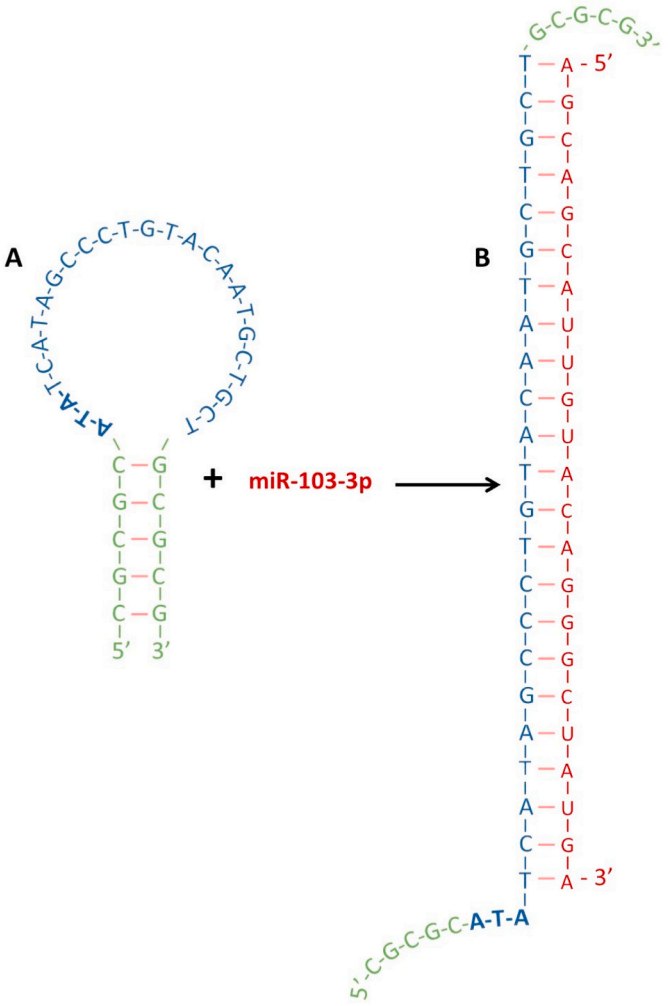

Fig. 3. Hybridization of Molecular Beacon probe (MB). A) Folding of the MB designed for miR-103–3p, ΔG = −5.75 kcal/mol. In green is the stem of the MB. In blue, the loop of the MB and bases in bold were added to the target sequence to allow the correct folding of the MB, quenching the fluorophore in the absence of the target. B) Spontaneous hybridization at room temperature of MB probe to the target, ΔG = −30.9 kcal/mol. In blue is the loop of the MB probe, in green is the stem of the MB probe, and in red is the miR-103–3p target.

constructed a calibration curve by serial dilutions of synthetic miR-103–3p in TE by qRT-PCR (Fig. 5). The graph (Fig. 5) shows the linear relationship between Ct values and serial dilutions of miR-103–3p with a coefficient of determination ($R^2 = 0.98$). Comparing calibration curves in TE for both microgels assay and qRT-PCR, we have a straight line and the same coefficient of correlation ($R^2 = 0.98$) (Fig. S3 and Fig. 5). Meanwhile, amplification failed when we performed qRT-PCR on samples spiked with 10 nM of miR-103–3p. We determined the limit of detection (LOD) of the microgels assay in TE buffer being about 100 fM using the method of the limit of Blank [39]. The LOD of qRT-PCR was considered the minimum concentration of nucleic acid, which always gives a positive PCR result in all replicates tested [41], and was identified at Ct > 29 in this assay. We conclude that the microgels assay provides a linear response as qRT-PCR for miRNAs quantification in TE. Moreover, we demonstrate that the microgels assay has a higher dynamic range (100 fM – 10 nM) than qRT-PCR in real samples without protocol rearrangement.

At this point, we tested the performances of both assays to detect miRNAs from serum samples. We aimed to evaluate the effect of interferent molecules that may be co-purified with miRNAs from a real sample. Both microgels assay and qRT-PCR were used to detect miR-

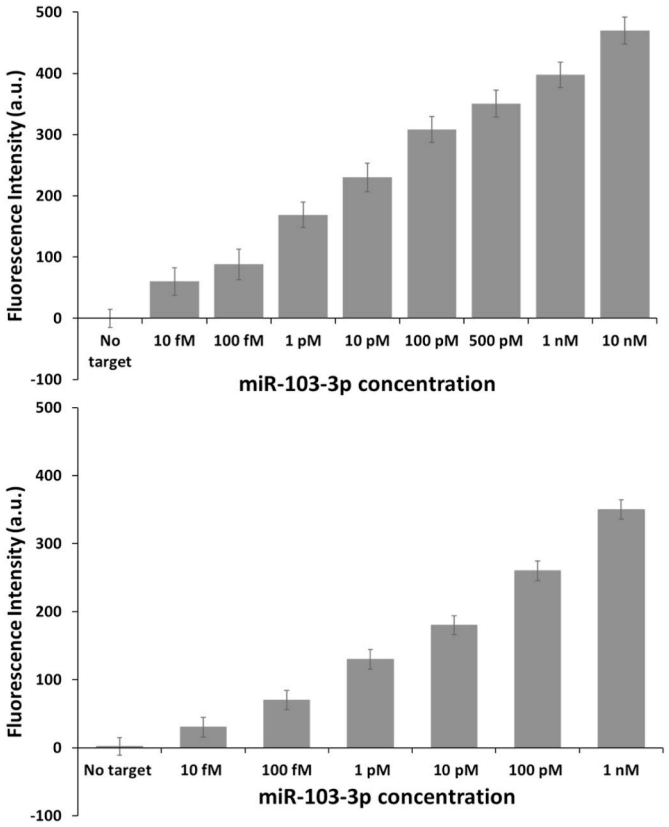

Fig. 4. Performance of microgel assay in detecting miR-103–3p in serum samples. A) Serial dilutions of miR-103–3p (10 fM – 10^6 fM) in Tris-EDTA (TE) detected by microgels assay were performed to calibrate the assay. B) Determination of miR-103–3p in serum samples. Three different spiked samples (biological replicates) were tested for each concentration; the results represent the mean of three different technical replicates for each sample. Error bars are SEM (standard error of the mean). 'No target' in the x-axis represents condition where microgels are in TE without miR-103–3p target.

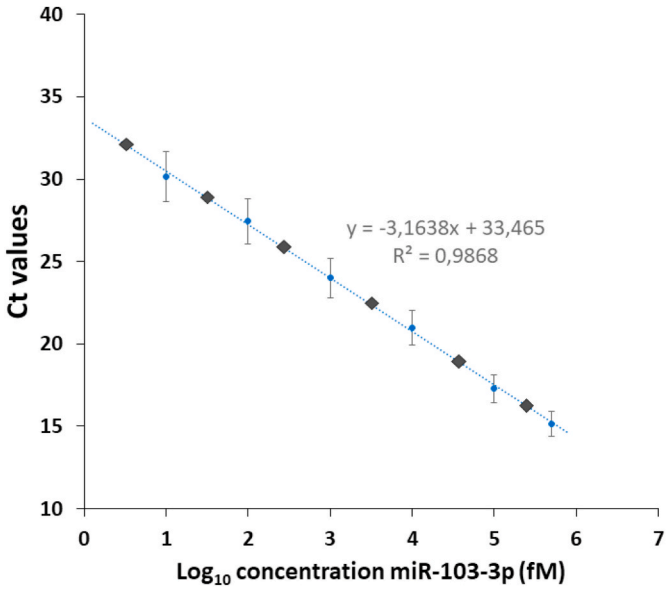

Fig. 5. Performance of qRT-PCR in detecting miR-103–3p in the serum samples. qRT-PCR was performed on serial dilutions of miR-103–3p in Tris-EDTA (TE) to create a calibration curve of the assay. The calibration curve was created using the following concentration of miR-103–3p (10 fM – 10^5 fM and 500 fM as the last point).

103–3p spike-in at defined concentrations in serum samples.

By microgels assay, in serum samples, we observed a lower fluorescence recovery comparing the same concentrations on the calibration curve in TE (Fig. 4B). However, by qRT-PCR in serum samples, we also observed an increase of about two cycles than the same concentrations on the calibration curve in TE (Fig. 5 and Fig. S5). The same results were observed by normalizing the data on the endogenous control miR-16–5p detected in serum samples by qRT-PCR together with miR-103–3p (Fig. S4). Moreover, using the qRT-PCR manufacturer's protocol for miR-103–3p detection in serum, we have a 'hook-affect' in the shape of the amplification curve (Fig. S5) meaning that fluorescence values decrease following an initial amplification phase. The 'hook effect' may be due to the errors during denaturation and annealing cycles of amplification [42], bringing false-negative results. For both assays, the lower signal detected in serum samples compared to TE is due to not fully complete recovery of RNA from serum samples that typically affect the column extraction kit [43]. From the analyses in serum samples, we can conclude that off-target miRNAs or other biomolecules do not interfere with signal transduction of microgels assay giving false results in real samples. Moreover, microgels assay, not foreseeing, denaturation, and annealing cycles do not incur in "hook effect" and is more reliable than qRT-PCR, mostly at high concentrations.

To further validate microgels assay in real samples, we compared the detection of circulating miR-103–3p in cancer cells (MCF7 media) with qRT-PCR. To explore the complexity of the MCF7 media, we performed qRT-PCR to detect both miR-103–3p and a set of miRNAs selected from the literature among the most overexpressed in MCF7 cells (Fig. 6A). As shown in (Fig. 6B), in MCF7 media we detected by qRT-PCR others miRNAs more expressed than miR-130–3p. The analyses by microgels assay in MCF7 media demonstrate its capability to specifically detect a low expressed miRNA (Ct of qRT-PCR ~29) in real samples and in the presence of more expressed miRNAs (Fig. 6B and C). Additionally, to confirm that microgels assay specifically detects miR-103–3p in MCF7 media (Fig. 6C), we tested MCF7 media in which no cells were cultured with the addition of a synthetic miRNA (miR-21) with a non-matching sequence to MB, in this, we didn't observe fluorescence emission. So, microgels assay can detect low abundant miRNAs in real samples, having good sensitivity compared to qRT-PCR. Both assays, qRT-PCR and microgels assay detect the same concentration of approximately 100 fM in MCF7 cells sample (Fig. S6). Moreover, we want to underline that each round of PCR doubles the amount of target starting material at each cycle, so at Ct~29, qRT-PCR fluorescence detection is performed on a larger amount of material than the starting one in MCF7 media. By qRT-PCR, we can detect miR-103–3p in the femtomolar range following 29 cycles of amplification (Table S4), after which we have 2^{43} more copies of the miRNA. Conversely, microgel assay directly detects the low amount of miR-103–3p without amplifying the starting material, which avoids the challenges of PCR inhibition. This is achievable thanks to the confinement of the target miR-103–3p on microgels that enhance fluorescence signal [36].

miRNAs detection is challenging for their low abundance and also for their sequence similarity, so the specificity evaluation is crucial to define the quality of a new assay. qRT-PCR is usually specific for single nucleotide polymorphisms (SNPs) but has the issue of off-target sequences. In SNP genotyping, these events can lead to false negative or false positive calls, complicating analyses and reducing confidence in results [44]. Microgels assay being amplification-free can improve the reliability of SNPs detection compared to qRT-PCR. To this end, we tested microgels' capability to discriminate SNPs in the target sequence. We performed microgels assay using miR-107 as a synthetic target. miR-107 belongs to the same miRNAs family as miR-103–3p; consequently, it shares with miR-103–3p all but one of the target nucleotides. A further test with microgels assay was performed using a synthetic oligonucleotide bearing two SNPs in the target sequence. We observe a decrease in the fluorescence signal in the presence of one SNP and two SNPs compared to the microgels assay performed with wild-type (WT) miR-103–3p. This demonstrates that the probe correctly hybridizes to the target only in a wild-type sequence, thus recognizing mismatched targets (Fig. S7). We can conclude that microgels assay represents a valid and advantageous alternative for miRNAs quantification and discrimination advantages over qRT-PCR, being amplification-free and time-saving.

5. Conclusions

In this work, we test microgels assay in the presence of multiple factors that are recognized as affecting the performance of qRT-PCR. We prove that microgels assay reaches a high sensitivity (fM) in real

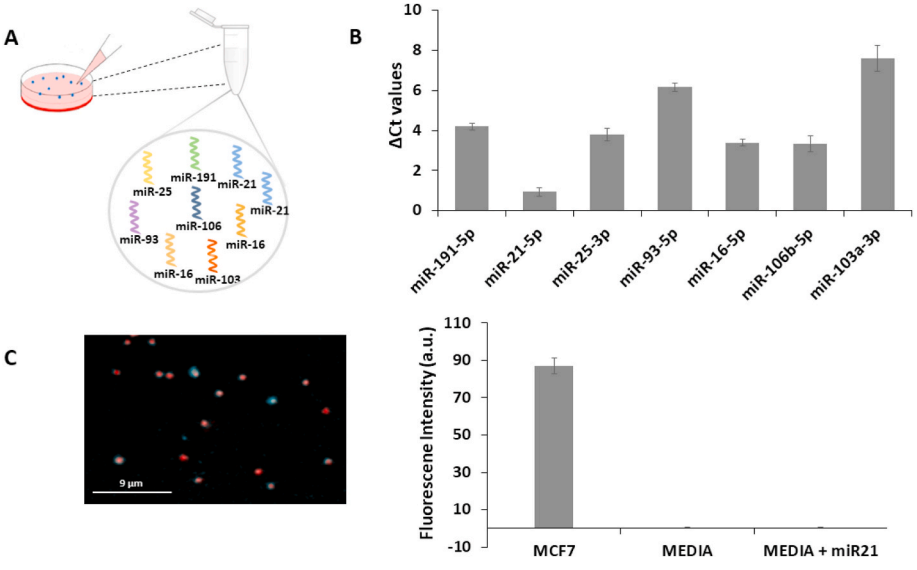

Fig. 6. miRNA-103–3p detection in real samples to validate the microgels-based assay. A) Graphical representation of the real sample (MCF7 cells media) used to perform miR-103–3p analysis with the TaqMan qRT-PCR assay and with the microgels-based assay. The miRNAs listed in the test tube are those screened by TaqMan qRT-PCR (Fig. 6B) to evaluate the presence in the real sample of over-expressed miRNAs other than miR-103–3p. B) ΔCt values of the pool of circulating miRNAs listed in Fig. 6A, miRNAs were detected in MCF7 cells media using TaqMan qRT-PCR assay. ΔCt for each miRNA in the graph was obtained by normalizing the mean of the values of Ct of each miRNA on the mean of the values of Ct of an exogenous control Cel-miR-39–3p (Table S4). C) Microgels-based assay for miR-103–3p in MCF7 cells media. In the confocal image are shown microgels following miR-103–3p detection. In blue is, the fluorophore of the molecular beacon, (Atto647N) in red is the fluorophore of the microgels (ATTO532). The graph shows microgels assay quantifying circulating miR-103–3p in cell culture media from MCF7 cells. MCF7: is media taken from MCF7 cell culture. MEDIA: cell culture media in which no cells were cultured. MEDIA + miR-21: cell culture media in which no cells were cultured and with the addition of 3 µL di 1 nM synthetic miR-21. Error bars are SEM. ΔCt: Delta Cycle threshold. SD: Standard Deviation. CV: Coefficient of Variation. SEM: Standard Error of the Mean. All values are expressed as the mean of at least three independent experiments (each sample was tested in triplicate).

biological samples and maintains a good selectivity without interference from other over-expressed miRNAs. It is also adaptable to a broader range of concentrations without protocol optimization. In contrast, for qRT-PCR at higher concentrations, we observe a "hook-effect" in the curve shape that can affect the results. The proposed assay is easily performed with a small amount of biological sample (2 μL) in a volume as that of qRT-PCR (20 μL) at 25 °C. We demonstrate that it can be performed directly in RNA extracts. A small amount of target can also be detected in the presence of more concentrated miRNAs in the same sample with high specificity.

In conclusion, microgels assay represents a feasible tool to improve discrepancy in the results of current methods based on laborious and time waste sample preparations and target amplification. Thanks to its analytical capabilities, microgels assay can satisfy the need for a fast and amplification-free method to validate the findings in which current methods are yet affected by false positive and false negative errors. Therefore, this method can open the venue for creating an array for multiplex screening of different miRNAs, as for several classes of biomarkers with which current detection methods are hardly dealing. The system also has the potential to be further integrated and validated using a microfluidic approach for ultrasensitive miRNA detection directly in biological fluids, and this will also eliminate the RNA extraction steps.

Credit author statement

Sabrina Napoletano: investigation, methodology, data curation, formal analysis, writing - original draft, writing - review and editing. **Edmondo Battista:** investigation, writing – review, and editing. **Nicoletta Martone:** investigation, methodology, writing - review, and editing. **Paolo Antonio Netti:** writing - review and editing; **Filippo Causa:** conceptualization, project administration, supervision, writing - review and editing, funding acquisition.

The manuscript was written through the contributions of all authors. All authors have approved the final version of the manuscript.

Author agreement

All authors have approved the final version of the manuscript being submitted. The article is original work and has not received prior publication and is not under consideration for publication elsewhere.

Declaration of competing interest

The authors declare the following financial interests/personal relationships which may be considered as potential competing interests: Filippo Causa reports financial support was provided by Italian Association for Cancer Research. Filippo Causa reports a relationship with Italian Association for Cancer Research that includes: funding grants.

Data availability

Data will be made available on request.

Acknowledgements

The authors acknowledge financial support from the AIRC (Fondazione Italiana Ricerca sul Cancro), IG Grant n. 24623.

The authors would like to thank Bianca Maria Nastri for her support in arranging data for microgel assay in TE.

Appendix A. Supplementary data

Supplementary data to this article can be found online at https://doi.org/10.1016/j.talanta.2023.124468.

References

[1] S. Anfossi, A. Babayan, K. Pantel, G.A. Calin, Clinical utility of circulating non-coding RNAs - an update, Nat. Rev. Clin. Oncol. 15 (2018) 541–563.
[2] O.F. Quirico L, The Power of microRNAs as Diagnostic and Prognostic Biomarkers in Liquid Biopsies, Cancer Drug Resist, 2020, pp. 117–139.
[3] H. Liu, Q.Z. Bian, W. Zhang, H.B. Cui, Circulating microRNA-103a-3p could be a diagnostic and prognostic biomarker for breast cancer, Oncol. Lett. 23 (2022) 38.
[4] P. Leidinger, C. Backes, S. Deutscher, K. Schmitt, S.C. Mueller, K. Frese, J. Haas, K. Ruprecht, F. Paul, C. Stähler, C.J. Lang, B. Meder, T. Bartfai, E. Meese, A. Keller, A blood based 12-miRNA signature of Alzheimer disease patients, Genome Biol. 14 (2013) R78.
[5] M. Vijayan, P.H. Reddy, Peripheral biomarkers of stroke: focus on circulatory microRNAs, Biochim. Biophys. Acta 1862 (2016) 1984–1993.
[6] J. Cacheux, A. Bancaud, T. Leichlé, P. Cordelier, Technological challenges and future issues for the detection of circulating MicroRNAs in patients with cancer, Front. Chem. 7 (2019) 815.
[7] C.C. Pritchard, H.H. Cheng, M. Tewari, MicroRNA profiling: approaches and considerations, Nat. Rev. Genet. 13 (2012) 358–369.
[8] B. Martinez, P.V. Peplow, MicroRNAs as diagnostic and therapeutic tools for Alzheimer's disease: advances and limitations, Neural Regen Res 14 (2019) 242–255.
[9] L. Mompeón, X. Ortega-Paz, , Vidal-Gómez, T.J. Costa, D. Pérez-Cremades, S. Garcia-Blas, S. Brugaletta, J. Sanchis, M. Sabate, S. Novella, A.P. Dantas, C. Hermenegildo, Disparate miRNA expression in serum and plasma of patients with acute myocardial infarction: a systematic and paired comparative analysis, Sci. Rep. 10 (2020) 5373.
[10] K. Saliminejad, H.R. Khorram Khorshid, S.H. Ghaffari, Why have microRNA biomarkers not been translated from bench to clinic? Future Oncol. 15 (2019) 801–803.
[11] J.F. Huggett, T. Novak, J.A. Garson, C. Green, S.D. Morris-Jones, R.F. Miller, A. Zumla, Differential susceptibility of PCR reactions to inhibitors: an important and unrecognised phenomenon, BMC Res. Notes 1 (2008) 70.
[12] D.A. Forero, Y. González-Giraldo, L.J. Castro-Vega, G.E. Barreto, qPCR-based methods for expression analysis of miRNAs, Biotechniques 67 (2019) 192–199.
[13] N. Minshall, A. Git, Enzyme- and gene-specific biases in reverse transcription of RNA raise concerns for evaluating gene expression, Sci. Rep. 10 (2020) 8151.
[14] Ruiz-Villalba, J.M. Ruijter, M.J.B. van den Hoff, Use and Misuse of Cq in qPCR Data Analysis and Reporting, Life (Basel), 2021, p. 11.
[15] S.A. Bustin, T. Nolan, Pitfalls of quantitative real-time reverse-transcription polymerase chain reaction, J. Biomol. Tech. 15 (2004) 155–166.
[16] R. Alaeddini, Forensic implications of PCR inhibition–A review, Forensic Sci Int Genet 6 (2012) 297–305.
[17] M. Sidstedt, P. Rådström, J. Hedman, PCR inhibition in qPCR, dPCR and MPS-mechanisms and solutions, Anal. Bioanal. Chem. 412 (2020) 2009–2023.
[18] D.J. Kim, S. Linnstaedt, J. Palma, J.C. Park, E. Ntrivalas, J.Y. Kwak-Kim, A. Gilman-Sachs, K. Beaman, M.L. Hastings, J.N. Martin, D.M. Duelli, Plasma components affect accuracy of circulating cancer-related microRNA quantitation, J. Mol. Diagn. 14 (2012) 71–80.
[19] C. Schrader, A. Schielke, L. Ellerbroek, R. Johne, PCR inhibitors - occurrence, properties and removal, J. Appl. Microbiol. 113 (2012) 1014–1026.
[20] A.R. Chandrasekaran, J.A. Punnoose, L. Zhou, P. Dey, B.K. Dey, K. Halvorsen, DNA nanotechnology approaches for microRNA detection and diagnosis, Nucleic Acids Res. 47 (2019) 10489–10505.
[21] I.S. Sourvinou, A. Markou, E.S. Lianidou, Quantification of circulating miRNAs in plasma: effect of preanalytical and analytical parameters on their isolation and stability, J. Mol. Diagn. 15 (2013) 827–834.
[22] J. Murphy, S.A. Bustin, Reliability of real-time reverse-transcription PCR in clinical diagnostics: gold standard or substandard? Expert Rev. Mol. Diagn 9 (2009) 187–197.
[23] A. Ardebili Tahamtan, Real-time RT-PCR in COVID-19 detection: issues affecting the results, Expert Rev. Mol. Diagn 20 (2020) 453–454.
[24] J.S. McDonald, D. Milosevic, H.V. Reddi, S.K. Grebe, A. Algeciras-Schimnich, Analysis of circulating microRNA: preanalytical and analytical challenges, Clin. Chem. 57 (2011) 833–840.
[25] A.E. Bilgrau, S. Falgreen, A. Petersen, M.K. Kjeldsen, J.S. Bødker, H.E. Johnsen, K. Dybkær, M. Bøgsted, Unaccounted uncertainty from qPCR efficiency estimates entails uncontrolled false positive rates, BMC Bioinf. 17 (2016) 159.
[26] J. Qin, W. Wang, L. Gao, S.Q. Yao, Emerging biosensing and transducing techniques for potential applications in point-of-care diagnostics, Chem. Sci. 13 (2022) 2857–2876.
[27] F. Precazzini, S. Detassis, A.S. Imperatori, M.A. Denti, P. Campomenosi, Measurements methods for the development of MicroRNA-based tests for cancer diagnosis, Int. J. Mol. Sci. 22 (2021).
[28] U. Bora, A. Sett, D. Singh, Nucleic Acid Based Biosensors for Clinical Applications, Biosens. J., 2013, pp. 1–8.
[29] R. Tavallaie, S.R. De Almeida, J.J. Gooding, Toward Biosensors for the Detection of Circulating microRNA as a Cancer Biomarker: an Overview of the Challenges and Successes, vol. 7, Wiley Interdiscip Rev Nanomed Nanobiotechnol, 2015, pp. 580–592.
[30] E. Xiong, D. Zhen, L. Jiang, Homogeneous enzyme-free and entropy-driven isothermal fluorescent assay for nucleic acids based on a dual-signal output amplification strategy, Chem Commun (Camb) 54 (2018) 12594–12597.
[31] C.Y. Hong, X. Chen, T. Liu, J. Li, H.H. Yang, J.H. Chen, G.N. Chen, Ultrasensitive electrochemical detection of cancer-associated circulating microRNA in serum samples based on DNA concatamers, Biosens. Bioelectron. 50 (2013) 132–136.

[32] H.N. Chan, S.L. Ho, D. He, H.W. Li, Direct and sensitive detection of circulating miRNA in human serum by ligase-mediated amplification, Talanta 206 (2020), 120217.
[33] T. Kangkamano, A. Numnuam, W. Limbut, P. Kanatharana, T. Vilaivan, P. Thavarungkul, Pyrrolidinyl PNA polypyrrole/silver nanofoam electrode as a novel label-free electrochemical miRNA-21 biosensor, Biosens. Bioelectron. 102 (2018) 217–225.
[34] F. Hakimian, H. Ghourchian, Ultrasensitive electrochemical biosensor for detection of microRNA-155 as a breast cancer risk factor, Anal. Chim. Acta 1136 (2020) 1–8.
[35] J.F. Masson, Consideration of sample matrix effects and "biological" noise in optimizing the limit of detection of biosensors, ACS Sens. 5 (2020) 3290–3292.
[36] F. Causa, A. Aliberti, A.M. Cusano, E. Battista, P.A. Netti, Supramolecular spectrally encoded microgels with double strand probes for absolute and direct miRNA fluorescence detection at high sensitivity, J. Am. Chem. Soc. 137 (2015) 1758–1761.
[37] T.M. Caputo, E. Battista, P.A. Netti, F. Causa, Supramolecular microgels with molecular beacons at the interface for ultrasensitive, amplification-free, and SNP-selective miRNA fluorescence detection, ACS Appl. Mater. Interfaces 11 (2019) 17147–17156.
[38] D. Dannhauser, F. Causa, E. Battista, A.M. Cusano, D. Rossi, P.A. Netti, In-flow real-time detection of spectrally encoded microgels for miRNA absolute quantification, Biomicrofluidics 10 (6) (2016), 064114.
[39] D.A. Armbruster, T. Pry, Limit of blank, limit of detection and limit of quantitation, Clin. Biochem. Rev. 29 (Suppl 1) (2008) S49–S52.
[40] D. de Gonzalo-Calvo, M. Sopić, Y. Devaux, E.-C.C.A. CA17129, Methodological considerations for circulating long noncoding RNA quantification, Trends Mol. Med. 28 (2022) 616–618 (K).
[41] Warton, Y. Xu, C.E. Ford, Target sequence heterogeneity causes the 'hook effect' in fluorescent dye-based quantitative PCR, Biotechniques 69 (2020) 80–83.
[42] P. Kralik, M. Ricchi, A basic guide to real time PCR in microbial diagnostics: definitions, parameters, and everything, Front. Microbiol. 8 (2017) 108.
[43] M. Husakova, P. Kralik, V. Babak, I. Slana, Efficiency of DNA isolation methods based on silica columns and magnetic separation tested for the detection of, Materials 13 (2020).
[44] T. Ouyang, Z. Liu, Z. Han, Q. Ge, MicroRNA detection specificity: recent advances and future perspective, Anal. Chem. 91 (2019) 3179–3186.